SYSTEMATIC STUDIES OF THE SECOND SOUND METHOD FOR QUENCH DETECTION OF SUPERCONDUCTING RADIO FREQUENCY CAVITIES

L. Steder*, B. Bein, W. Hillert[1], D. Reschke, DESY, Hamburg, Germany
[1] also at University of Hamburg, Germany

Abstract

DESY conducts research and development for superconducting radio frequency cavities. One part of the manifold activities are vertical performance tests. Besides the determination of accelerating gradient and quality factor, additional sensors and diagnostic methods are used to obtain more information about the cavity behaviour and the test environment. The second sound system is a tool for spatially resolved quench detection via oscillating super-leak transducers, they record the second sound wave, generated by the quench of the superconducting Niobium. The mounting of the sensors was improved to reduce systematic uncertainties and results of a recent master thesis are presented in the following. Different reconstruction methods are used to determine the origin of the waves. The precision, constraints and limits of these are compared. To introduce an external reference and to qualify the different methods a calibration tool was used. It injects short heat pulses to resistors at exact known space and time coordinates. Results obtained by the different algorithms and measurements with the calibration tool are presented with an emphasis on the possible spatial resolution and the estimation of systematic uncertainties of the methods.
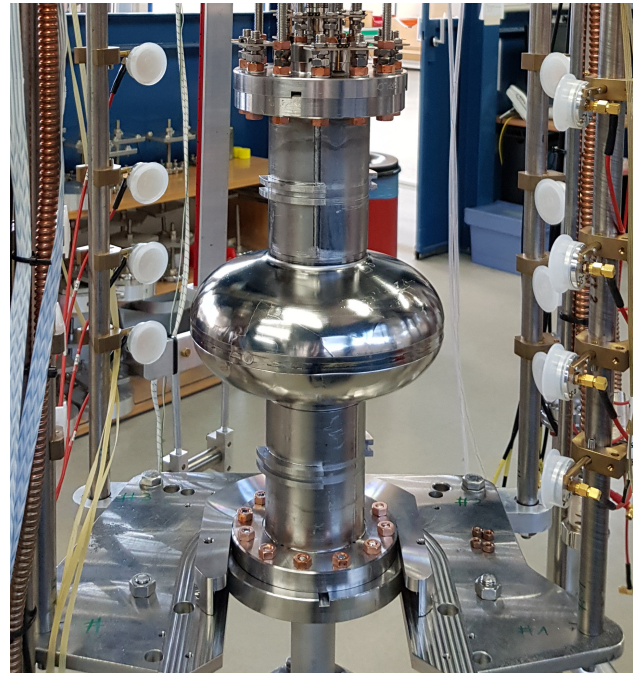
Figure 1: Single-cell cavity in R&D insert equipped with OST sensors for second sound quench localisation. The membranes of the OSTs are protected against mechanical impact by white caps.

SECOND SOUND METHOD FOR QUENCH LOCALISATION

Second sound waves are temperature-driven entropy waves in the liquid Helium produced during a local thermal or magnetic breakdown (quench) of the superconductivity at the inner cavity surface [1]. Oscillating super-leak transducers (OSTs) [2] are able to detect the waves. They work like a microphone using the Brass body and a porous membrane as capacitor and utilising the fact, that only the superfluid He II phase is able to pass the small pores. With the run-times deduced from the OST signals, the position of the OSTs and the second sound velocity in liquid Helium, the quench-spot can be reconstructed. For this purpose multiple algorithms employing two different approaches are used.

In the following, upgrades of the hardware installation, the automation of the data analysis, a comparison of the algorithms and first tests towards an external calibration of the quench localisation system are given. The here presented work is a summary of a recently finished master thesis [3].

Realisation of Second Sound System at DESY

At DESY all vertical cavity performance tests are performed in the Accelerator Module Test Facility (AMTF). For R&D purposes two inserts are available to mount a single –typically 1.3 GHz TESLA type– cavity with surrounding diagnostic systems like temperature sensors, magnetic field sensors and OSTs to detect second sound waves.

In Figure 1, a single-cell superconducting radio frequency (SRF) cavity mounted in one of the R&D inserts is shown. The OST sensors can be recognised via their white caps preventing damage of the sensitive membrane. Those caps are only removed for the actual test. Brass holders are used to mount the OSTs to the four existing support rods of the insert. In order to provide well known and reproducible positions of the OST sensors, milled notches in the rods at the equator positions of single- and nine-cell TESLA cavities are introduced. These allow a placement accuracy after dismounting and mounting of the OSTs of about 1 mm over all Cartesian coordinates.

---

* lea.steder@desy.de

SURFACE COVERAGE AND SYMMETRIC INSTALLATION

In order to overcome the necessity to dismount the OSTs every time the cavity is exchanged, at each supporting rod all OST holders are placed at one side. This results in a gap between the OSTs, large enough to assemble cavities into the insert. In consequence, a new OST assembly is only needed when a single-cell cavity is replaced by a nine-cell cavity or the other way round. This mounting strategy improves the precision of the OST positioning even further, which was enhanced before by the milled notches.

Surface Coverage

In [3] the coverage of the cavity surface by the OST sensors visibility fields was analysed. The result can be seen in Figure 2. Apparently, in the front at coordinates $(0, -100)$
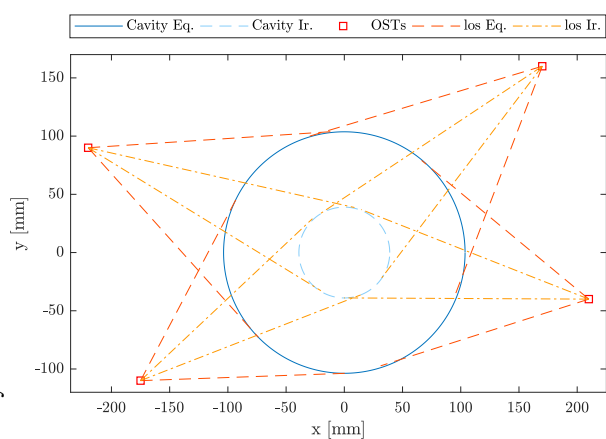

Figure 2: XY-cut through cavity equator. In dark blue the equator circumference is shown, while light blue depicts the beam tube. The orange boxes represent the OST sensors and the dashed lines illustrate the visibility fields of the OSTs.

and on the back $(0, 100)$ of the cavity areas exist, which are almost or even not at all covered by OST sensors. Obviously the idea to reduce the need of OST assemblies via the new mounting strategy yields an insufficient coverage of the cavity surface by OSTs.

In order to get rid of that problem an additional holder system was designed and is fabricated at the moment. Those new holders will enable OST positioning in front of the mentioned blind spots, resulting in a full coverage of the cavity surface. Some of these new holders will have to be dismounted every time the cavity is exchanged.

Symmetric Installation

In the DAQ system for the OST signals 18 channels are available, which means that for each test of a single- or nine-cell cavity 18 OSTs can be placed around the cavity. For nine-cell cavities two OSTs are mounted at each of the different equator heights. In case of the here studied single-cell cavities, four installation layers are used. One at the exact equator height and two layers in symmetrical distance above

and below the equator. Since more channels are available, an additional layer of OSTs on top of the other three is installed as it can be seen in figures 1 and 3.
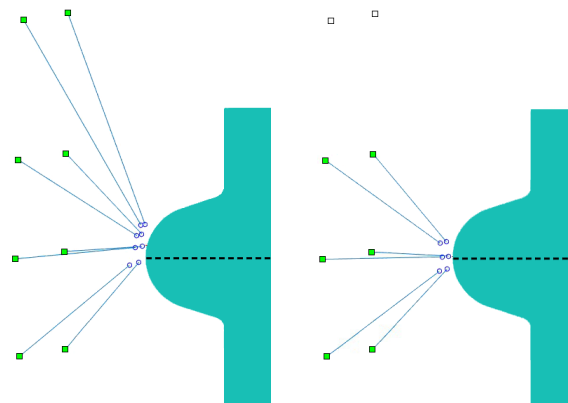

Figure 3: Quench-spot reconstruction with all 4 (left) and only the 3 symmetric line-of-sight OST layers. Green squares depict positions of used OSTs. Blank squares represent OSTs not contributing to the reconstruction. Signals are taken from cavity 1DE27 test 1. Due to the not exactly fitting distances, the reconstructed quench-spots are moved towards centre-of-mass of all used OSTs. A difference in the z coordinate of 8 mm is the result.

The signal run-time deduction is described in the next section. Sometimes the run-times are not perfectly matching the distance between quench-spot and OST sensor. In such cases, the reconstruction algorithms move the calculated quench origin towards the centre-of-mass of all used OSTs. In the left part of Figure 3, the asymmetric configuration together with the slightly too short run-times produce a shift of 8 mm in height. The quench-spot is due to the usage of all available OST signals artificially shifted away from the equator (dashed black line).

In consequence an asymmetric positioning of the OST sensors has to be avoided, since it is able to introduce a bias of the reconstructed quench position.

DATA ANALYSIS PROCESS

The quench detection via second sound measurements can be subdivided in three steps. First of all the quench-time t_0 has to be determined, as well as the signal run-times t_{OST_i}. Then the exact positions of the OST sensors have to be implemented and the propagation velocity of the second sound wave has to be deduced from the liquid Helium temperature. In the end follows the quench spot reconstruction using the deduced times and configuration parameters. For this last step different algorithms can be used.

In the scope of a master thesis [3] the complete chain of data analysis was revised. Existing codes were implemented in a common framework based on Matlab. Many additional algorithms for automation were added and graphical user interfaces (GUI) were written. In the following, all above mentioned steps are described briefly, further details can be found in [3].

Noise Filtering

Since the noise level of all acquired OST signals is quite high, improvements on the hardware side are implemented via a more stable power supply, an improved line filter and an advanced amplifier circuit. Activities in this direction will last further, since still a non-negligible amount of noise is present.

Software-wise a noise filtering has to be applied on the raw data of the OST signals. The unfiltered Fourier spectrum shows large peaks at 50 Hz and higher odd harmonics of 50 Hz. Hence, a Notch filter is applied to filter those frequencies. The effect of this filtering can be seen in Figure 4 comparing the upper and lower plot.

Quench-Time Deduction

In order to define the starting point of the second sound wave propagation the quench-time t_0 has to be deduced. For this purpose the characteristic radio frequency (RF) signals, i.e. transmitted power to the probe antenna and reflected power at the input antenna of the cavity, are used. During the quench the reflected signal shows a sudden increase, while the transmitted signal dissipates.

For an automated detection of t_0, the slope of both signals are convoluted with a step function: a 1 is assigned at regions showing a slope, in case of no existing slope a 0 is allocated. Afterwards the results are multiplied in order to eliminate regions, in which only one of the signals is increasing or decreasing. The left edge of the non-zero region in the binary convolution is defined as the time of the quench.

Signal Run-Time Deduction and Selection

Goal of the sequence is to find the first clear peak in the signal which describes the response of the OST membrane to the second sound wave. With the knowledge of the quench-time the signal run-time can be calculated and used for the quench-spot reconstruction. Using the liquid Helium temperature and thus the propagation velocity u_2 of the wave the distance can be calculated for a given signal run-time.

As input for the determination of signal run-times both filtered and unfiltered signals are used, they can be seen in Figure 4. Since both signals are independently processed by the signal time deduction, two lists of run-times are resulting.

A 6 σ environment is used as envelope for the noise and all peaks above this threshold get a signal quality assigned. This quality is simply defined by the ratio of the peak height to the maximal peak height in the given channel. Using the signal quality and a reduction of search windows in the overall 20 seconds long signals, an iterative process for the definition of the run-times is performed. The resulting list is then used to select the best possible run-times for each channel and to exclude outliers. Such uncorrelated run-times can for example be produced due to diffraction on insert parts or the cryostat wall and can not be used for reconstruction since the assumption of a sphere-like propagation is not holding true in such cases.
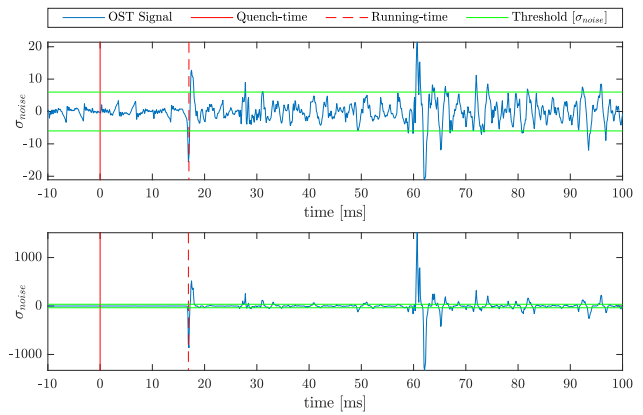

Figure 4: In the upper graph the unfiltered signal of one OST channel normalised to σ_{noise}, on the bottom the same signal after noise filtering is shown. The horizontal green lines are enveloping the noise and the vertical red lines mark the quench-time t_0, while the dashed red lines visualise the deduced signal-time t_{OST} of this very OST.

For this purpose, a first rough quench-spot has to be reconstructed using all run-times. The RMSE (Root Mean Square Error) value describes the precision of the calculated spot. In case, this RMSE value is larger than 25 mm for a single-cell cavity (50 mm for nine cells) the threshold is reduced to 25 mm to enable the following procedure also under difficult conditions. An iterative procedure only takes into account run-times with a difference of less than twice the RMSE value and reconstructs the quench origin again with the help of a simple multilateration. To prevent the exclusion of all run-times after some iterations, signals with less than 10 mm distance to the quench-spot are always taken into account.

After the reduction of both run-time lists, for each channel a decision has to be taken which of the two values will be used. Either the one deduced from the unfiltered or the one defined by the filtered signal. For this decision, the distances of both competing run-times to the rough reconstructed quench-spot are compared. The run-time producing the smaller distance to the reconstructed spot is selected, since it seems to describe the quench-spot better. In the end, a final list of signal-run times exists and a decision about the line-of-sight can be taken via a second and now optimised surface constrained multilateration reconstruction (described in the next section).

Before the algorithms, introduced in [3], for quench- and run-time deduction were established, all definitions of such times were performed "manually by eye". The automation saves a lot of time and ensures a stable and reproducible quality of the quench-time determination.

Graphical User Interfaces

An important part of the software project is the development of graphical user interfaces (GUIs), one of them can be seen in Figure 5. They provide an environment to define the OST configuration, add a potential cavity angle offset result-
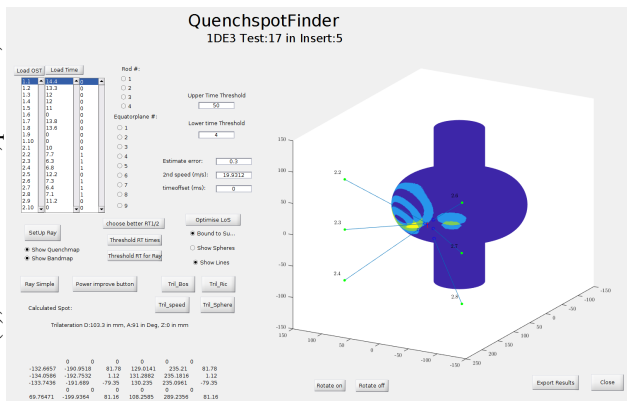
Figure 5: Exemplarily the graphical user interface for the last step of the reconstruction is shown. At this surface the actual quench-spot finding takes place.

ing from assembly in the insert and read the liquid Helium temperature from a database. Then a visualisation of all unfiltered and filtered signals with marked quench- and signal run-times for "manual" control are offered. And in a last step the quench-spot reconstruction is steered. OST signals can be selected or deselected and the reconstruction method can be chosen. In addition, the reconstructed quench-spots are displayed and, in the case of the raytracing algorithm (described in the section after the next), band- and quench-map are generated. The latter describe the reach of OST signals and the most probable position of the quench-spot on the cavity surface and are described as well in the section about the raytracing approach.

MULTILATERATION ALGORITHMS

Three or more by sensors measured signals can be used as starting points to reconstruct the unknown position of their origin. The measured distances can be drawn as spheres around their sensors (here: OSTs) and the resulting intersection of all the spheres defines, in case of second sound signals, the quench-spot location.

Three basic assumptions have to be made for the usage of multilateration for quench-spot localisation. First of all a constant second sound velocity in liquid Helium at given temperature. Second, a point-like origin and spherical propagation of the waves. And third, a direct line-of-sight between the quench-spot as wave origin and the OST for signal detection.

At DESY three different algorithms for multilateration are used and described in the following. All of them can be optionally used with an additional surface constraint, which requires that the reconstructed spot is forced to be a part of the surface function of the cavity.

Basic Multilateration

This reconstruction method does not presume more than the above mentioned conditions and is able to reconstruct the quench-spot everywhere, also off the cavity surface. At first glance, such a spot does not make sense, but several expla-

nation hypotheses for such an anomaly with a reconstructed spot above the cavity surface exist. The thermal conduction of Niobium can be one explanation, taking into account the fast propagation of the heat wave from the inner to the outer surface of the cavity [4]. Another model uses the response time of the reflected RF power, as described in [5]. And a third explanation incorporates the amplitude dependence of the second sound velocity. Since the wave is a temperature wave and the velocity is temperature dependent, the second sound signal is able to influence its own propagation velocity. More details about this effect can be found in [6, 7].

Technically, the distances calculated for all OSTs are fed into an error function of the spherical equations. The error function has to be minimised to determine the unknown quench-spot X. For X the already mentioned RMSE value can be calculated.

Velocity Fitting Multilateration

Expanding the basic algorithm, the distance of OST to quench-spot can be varied by the second sound velocity u_2 and the error function contains an additional unknown fit parameter. This idea is taking into account the above mentioned effect of the amplitude dependence of the second sound velocity.

Sphere Radius Fitting Multilateration

A third multilateration algorithm declines the second assumption for multilateration and allows for a spherical instead of a point-like wave source. This approach takes into account the distance of second sound wave origin on the outer cavity surface to the heat deposition on the inner surface. The calculated quench spot X is now the centre of a sphere with radius r, which is also included into the error function for minimisation.

The introduced radius r can also be interpreted as quench-time offset, further explanations as well as the exact definitions of the error functions for all algorithms can be found in [3].

RAYTRACING APPROACH

The approach of using all available OST signals via the so called raytracing algorithm was implemented at DESY some years ago. A thorough description can be found in [8]. Here, it shall only be mentioned that the cavity shape is simulated with the help of a mesh of vertices and edges stored in a graph and two more assumptions have to be added to the ones used for multilateration: The non line-of-sight OST signals are assumed to use always the shortest path through free space and on the cavity surface. For this purpose the graph is used to calculate geodesics on the surface. The second additional assumption fixes the quench origin intrinsically to the cavity surface.

Original Algorithm

In order to use the algorithm, the parametrised model of the cavity surface has to be calculated once and the spatial

OST configuration as well as the signal run-times have to be fed into the program. Outcome is a so called RMSE quench-map, which is a two-dimensional representation of the cavity surface. Shown is for each point consisting of height coordinate z' along the cavity surface and cavity angle ϕ an RMSE value. The position with the smallest RMSE value is assumed to be the quench-spot.

Line-of-Sight Raytracing and Band-Maps

In order to compare systematically the approaches of raytracing and multilateration, here an additional algorithm was implemented using only line-of-sight signals for the raytracing. With the implementation of this algorithm a better comparability of the multilateration and the raytracing approach is given.

In addition, a new representation for the results of the raytracing algorithms is defined. The so called band-maps, where the regions on the cavity surface are highlighted, which can be reached by the OST positions and their associated signal run-time. One example can be seen in the upper part of Figure 6.
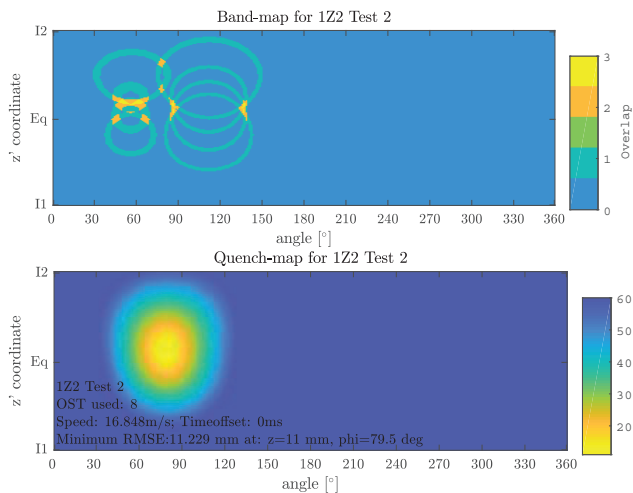

Figure 6: On the top, the band-map of test 2 of cavity 1Z2 is shown, for this reconstruction the algorithm only using line-of-sight signals is used. The axes depict the height z' along the surface of the cavity versus the angle. Colour-coded the overlap of the different OST-signals are visualised. The lower map represents the RMSE value for every point of the cavity surface.

The band-maps allow to decide about the quality of the reconstruction. At a glance, the number of overlapping OST signals for the assumed quench-spot is available.

Raytracing Observations

During the work presented here, a loss of spatial resolution in the quench-map was observed. The interpretation of the band-map shown in Figure 6 allows for three possible quench-spots, while the quench-map below clearly favours a single spot, which lies in between the others. For cross-

checks with optical inspections of cavity surfaces this loss of information is problematic.

A second observation is made comparing results of raytracing algorithms using all or only line-of-sight signal information. The distribution of quench-spots reconstructed by the original raytracing algorithm is much wider and does not match the distribution of quench-spots achieved with multilateration algorithms. A more thorough analysis of this indication has to follow.

INFLUENCE OF UNCERTAINTIES ON QUENCH-SPOT RECONSTRUCTION

In order to gain a realistic picture of the impact of systematic uncertainties on the spatial resolution of second sound quench-spot localisations two different approaches exist. First of all, a calibration of the complete reconstruction chain can be performed using an artificial heat deposition at well defined coordinates to simulate a quench event. The reconstructed origin of the so produced second sound waves can be compared with the real position and yields a precise resolution. This possibility will be discussed in the following section.

Another way to estimate the resolution of the above introduced algorithms is a simulation-based method. Starting point is a review of all possible sources for systematic uncertainties and the magnitude of their variations. In Table 1 these information are collected.

Table 1: Summary of Contributing Systematic Uncertainties for a Quench-spot Reconstruction

source		variations
OST position	x, y, z	1 mm
cavity position	x, y, z	3 mm
signal run-time	$t_{OST_i} - t_0$	0.2 ms
quench-time	t_0	0.5 ms
second sound velocity	u_2@2K	0.3 m/s
second sound velocity	u_2@1.8K	0.06 m/s
cavity length	z	3 mm

More explanations about the deduction of the summarised values and the following descriptions of the simulation methods can be found again in [3]. Worth mentioning here, are the two groups of variations. The upper half in the table deals with 3-dimensional influences, while the lower ones do affect only one dimension.

To simulate the influence of single parameters, real recordings of quench events are used. One individual parameter is smeared 250 times via a random distribution, of the in Table 1 given size, and the reconstruction is performed afterwards for all 250 variations. In the following, only multilateration algorithms are studied, since the simulation for raytracing is more complex.

The results for multilateration reconstructions with variations of OST position, cavity position and run-time can be seen in Figure 7.
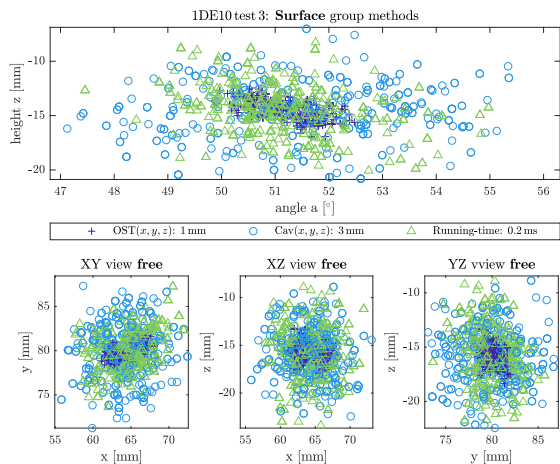
Figure 7: Result of uncertainty simulations for OST positioning (plusses), cavity positioning (circles) and signal run-time deduction (triangles). On the upper half algorithms reconstructing a quench-spot constrained to the cavity surface, in the lower line, three plots for reconstruction methods free of surface constraints are shown.
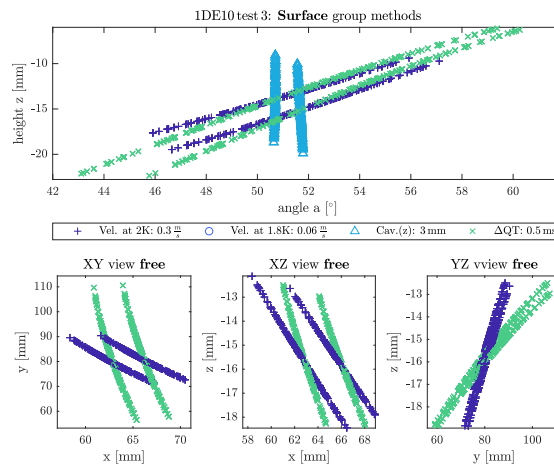

Figure 8: Result of simulation of two quench events smeared with uncertainties for second sound velocities at 2K (plusses) and 1.8K (circles), cavity height (triangles) and quench-time determination (crosses). On the upper half for algorithms which reconstruct a quench-spot constrained to the cavity surface. In the lower three plots for reconstruction methods free of surface constraints.

Since those are the 3-dimensional variations, cloud-like structures are produced. Different spreads can be observed, on the upper half of Figure 7 for surface constrained methods and on the lower for the unconstrained ones. In summary it can be stated, that a variation of the OST positions has only a small influence. The signal run-times impact is roughly twice as large. The cavity-position variation results in even larger spreads, which is not surprising given the assumed size of uncertainty (compare Table 1).

In Figure 8, the impact of one-dimensional variations of different parameters can be seen, they form trail-like structures. Two trails originating from two quench events are used for this uncertainty simulation.

In order to get more than a visual handle to interpret the results, the mean values of the standard deviations for all spatial coordinates are calculated afterwards for all algorithms [3].

On the one hand it can be stated, that the impact of the signal run-time variation is the largest. Hence, a precise as possible determination should be performed for all i run-times t_{OST_i}. The influence of the velocity of the second sound waves is on the other hand surprisingly low.

In the end, all parameters are smeared simultaneously to compare the robustness of the different algorithms. Most promising are the results of the surface constrained basic multilateration with a resolution of 6.6 mm $\pm$ 5.5 mm over both surface coordinates and the velocity fitting multilateration without a surface constraint with a resolution of 8.5 mm $\pm$ 2.8 mm over all three Cartesian coordinates.

EXTERNAL CALIBRATION

In order to achieve an even better basis to judge the quality of the used reconstruction algorithms an external calibration of the second sound system is preferable. With the help of reference measurements, realistic resolutions can be determined. The ability of the raytracing algorithm to enhance the resolution via the usage of OSTs, which are not in line-of-sight can be studied as well. In addition, geometrical effects can be analysed via sensible placement of the calibration signal.

To mimic a quench event, a heat pulse has to be induced into the liquid helium. For this purpose resistors are used. The spatial coordinates of such resistors have to be well known, afterwards the complete reconstruction chain can be evaluated via the reconstruction of this very spot.

Circuit boards were built and equipped with axial lead and SMD (surface mounted device) resistors of different types. Two of the boards are shown in Figure 9.
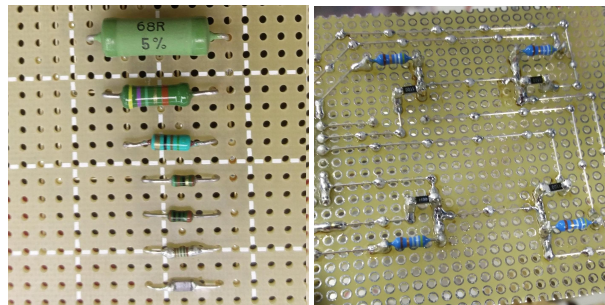

Figure 9: Two of the used resistor boards, on the left different axial lead resistors and on the right a geometrical layout also using SMD resistors for spatial resolution studies.

Those boards were mounted into the cavity inserts and after cool down to 2 Kelvin the resistors were pulsed in order to stimulate second sound wave emission. Due to not completely understood reasons only in very rare cases signals could be observed. And even then, they were not

visible in the raw data, but only after noise filtering, as it can be seen in Figure 10. One major role plays the noise level in the large cryostats in the AMTF environment. Signals were only observed in configurations with small distances to the OSTs. But over such short distances below 10 cm, the size of the OST membrane of 18 mm is not neglectable anymore and a spatial resolution of the second sound wave origin is not possible.
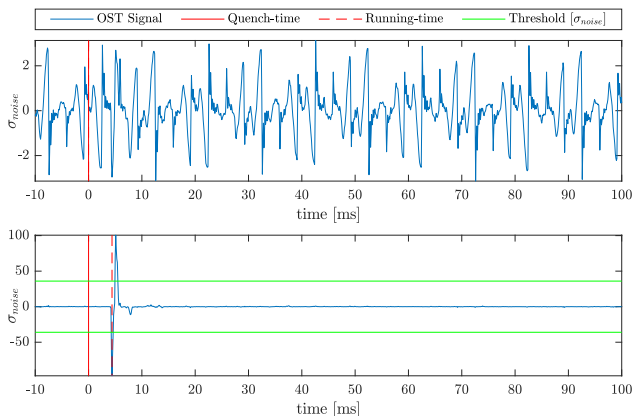

Figure 10: Unfiltered and noise filtered signal of an OST used during tests of the calibration resistors. The noise in the raw data hides the signal completely.

Many different configurations with varying distances to OSTs, different resistor types, variations of the supply voltage and circuit logic were tested. But none until now produced sufficient results, which really can be used to calibrate the quench localisation system. Hence, a collaboration concerning cavity diagnostic systems with INFN LASA in Milano was established and a new and more sophisticated tool for the calibration of second sound wave signals is under construction.

CONCLUSION

Lessons learned during systematic studies of the second sound method for quench detection of SRF cavities are first of all, that careful OST sensor positioning is very important. It has to be ensured, that all spots on the complete cavity surface are visible by at least three OSTs. In addition, a symmetric installation of OSTs around the cavity equator is of importance to avoid a bias in the geometric reconstruction of the quench-spot.

Another crucial point is the quality of the signal run-time determination, since the influence of variations of the run-time on the spatial resolution of the reconstruction is large. At DESY the sampling frequency could be raised and the noise-level should be improved further to achieve even better results for the signal run-times.

Concerning the different reconstruction algorithms, the basic multilateration with surface constraint and the velocity fitting multilateration without constraint produce the best resolutions below 10 mm. The validation of the raytracing algorithms is complicated and some questions concerning the usage of signals from OSTs not in line-of-sight with the quench-spot are still open.

Answers to those questions and an even deeper understanding of reconstruction methods will be enabled by the envisaged calibration system, which is at the moment under development at DESY.

ACKNOWLEDGEMENTS

REFERENCES

[1] R.J. Donnelly, "The Two-Fluid Theory and Second Sound in Liquid Helium," *Physics Today*, vol. 62, 2010. `doi:10.1063/1.3248499`

[2] Z. Conway, D. Hartill, H. Padamsee and E. Smith, "Defect Location in Superconducting Cavities Cooled with He-II Using Oscillating Superleak Transducers", in *Proc. PAC'09*, Vancouver, Canada, May 2009, paper TU5PFP044, pp. 921–923.

[3] B. Bein, "Systematic Studies of a Cavity Quench Localization System,", M.S. Thesis, DESY-THESIS-2019-010, University of Hamburg, 2019.

[4] Z. Liu, M. Kelly and A. Nassiri, "New method to improve the accuracy of quench position measurement on a superconducting cavity by a second sound method," *Phys. Rev. ST Accel. Beams*, vol. 15, p. 092001, 2012. `doi:10.1103/PhysRevSTAB.15.092001`

[5] R. Eichhorn and S. Markham, "On the Mystery of using Helium's Second Sound for Quench Detection of a Superconducting Cavity," *Phys. Procedia*, vol. 67, p. 822, 2015. `doi:10.1016/j.phpro.2015.06.138`

[6] A. Dessler and W.M. Fairbank, "Amplitude Dependence of the Velocity of Second Sound," *Phys. Rev.*, vol. 104, p. 6, 1956. `doi:10.1103/PhysRev.104.6`

[7] S. Markham, R. Eichhorn, D. Hartill and G. Hoffstaetter, "On Quench Propagation, Quench Detection and Second Sound in SRF Cavities", in *Proc. SRF'15*, Whistler, Canada, Sep. 2015, paper TUPB088, pp. 804–809.

[8] Y. Tamashevich, "Diagnostics and treatment of 1.3 GHz Nb cavities," Ph.D. thesis, University of Hamburg, Germany, 2016. `doi:10.3204/PUBDB-2017-00617`